NASA

Technical Memorandum 83923

A BROAD-BAND VLF-BURST ASSOCIATED WITH RING-CURRENT ELECTRONS

Kaichi Maeda

MARCH 1982

National Aeronautics and
Space Administration

Goddard Space Flight Center
Greenbelt, Maryland 20771

A Broad-Band VLF-Burst Associated with Ring-Current Electrons

Kaichi Maeda

Laboratory for Planetary Atmospheres

NASA/Goddard Space Flight Center

Greenbelt, MD 20771

March 1982

ABSTRACT

During the periods after the maximum phase of geomagnetic storms on 2 April 1972 a broad band VLF emission burst has been observed by the equatorially orbiting satellite S^3-A (Explorer 45) along its inbound plasmapause crossings. The frequency band broadening takes place just outside of the nighttime plasmasphere, where the density of cold plasma has been known to be very low (occasionally below 10 cm^{-3}) during the later phase of a geomagnetic storm. Instead of the gradual broadening of several hours duration, a burst type broadening of VLF emission lasting less than ten minutes was observed in the similar location. The magnetic field component of this emission is very weak and the frequency spreads below the local half electron cyclotron frequency. Corresponding enhancement of the anisotropic ring-current electrons is also very sudden and limited below the order of 10 keV without significant velocity dispersion, in contrast to the gradual broadening events. The cause of this type of emission band spreading can be attributed to the generation of the quasi-electrostatic whistler mode emissions of short wavelength by hot bi-maxwellian electrons surging into the domain of relatively low density magnetized cold plasma. The lack of energy dispersion in the enhanced electrons indicates that the inner edge of the plasma sheet, the source of these hot electrons, is not far from the location of this event.

1. INTRODUCTION

During the periods of geomagnetic disturbances, VLF-emissions associated with ring-current electrons have been observed by the equatorially orbiting small scientific satellite (S^3-A, Explorer 45) (Maeda, 1976; Anderson and Maeda, 1977). These VLF emissions were also observed by other satellites along their equatorial-crossing orbits outside of the nighttime plasmasphere (Burtis and Helliwell, 1969, 1976; Tsurutani and Smith, 1974). It was also noticed that the band of whistler mode emissions often spreads toward lower frequencies as the satellite approaches the nightside plasmapause. This gradual broadening of the whistler mode emission toward lower frequencies has been ascribed to the spreading of the pitch-angle anisotropy of the enhanced ring-current electrons towards higher energies (Maeda and Lin, 1981). The change in the anisotropy of energetic ring-current electrons is attributed to the combined effects of the E X B drift of the ring-current electrons from the geomagnetic tail and cross-magnetic field diffusions of these electrons injected from the earth's plasma sheet during periods of geomagentic disturbance (Kivelson and Southwood, 1975; Southwood and Kivelson, 1975; Maeda et al., 1978).

The purpose of this short article is, however, to describe another type of emission band broadening which has been observed by the S^3-A satellite in the similar location as those of gradually broadening emissions.

2. LOCATION OF THE EVENT

As indicated by a small square mark on the orbit just outside of the plasmasphere shown in Figure 1, the burst type VLF emission band broadening was observed by the S^3-A satellite on its inbound crossing of the plasmapause of the orbit 431. This event took place approximately at 04h UT on April 2,

1972, which is roughly at 20h geomagnetic local time. The K_p-indices at the previous 12 hours were 4-, 5, 3- and 5 (Lincoln, 1972), indicating that the event was observed in the late phase of a moderate geomagnetic storm. The plasmapause crossings and the estimated plasmasphere boundaries between the crossings are determined by the static electric field experiments of Maynard and Cauffman (1973).

3. THE EMISSION DATA

The wideband data of VLF emission obtained by the S^3-A satellite during the event are shown in Figure 2 where the upper and lower panel presents the magnetic field data and the electric field data, respectively. The instrumental upper cut-off frequency is 3 kHz for the magnetic field data (Parady et al., 1975) and 10 kHz for the electric field data (Anderson and Gurnett, 1973). The narrow band whistler mode emission with a gap along the half local electron cyclotron frequency, $f_H/2$, continued from its onset around 0403 UT. At $04^h10^m58^s$ UT, a sudden broadband type appeared spreading the band width from around $f_H/2$ (~ 5 kHz) to below 1 kHz. This short burst of emission ceased at $04^h\ 16^m\ 42^s$ UT as the satellite entered into the plasmasphere as shown in Figure 1. The broadening of this emission band below 3 kHz appears clearly in the electric field data but not significantly in the upper panel of magnetic field data, indicating that this broadened emission is a quasi-electrostatic mode, even though its frequency range extends below $f_H/2$. Insignificant magnetic field intensity of this broadband emission is not due to the effect of automatic gain control (AGC), nor due to the malfunction in the instrumental system for the following reasons: (1) AGC is not used in the AC magnetic field measurements but one of the three levels of amplification modes has been operating during the periods, including the present emission

event (L. J. Cahill, private communication, 1982). (2) As can be seen from Figure 2, a weak plasmaspheric hiss appears in the AC magnetic field data in frequency 1 - 0.5 kHz aroung 0423-0433 UT. (The inbound plasmapause crossing is approximately 0417 UT). (3) Based on the mode of operation and the information of instrumental sensitivity (Parady et al., 1975), the noise level of the AC magnetic field around 1000 Hz during the event is estimated to be of the order of 0.2 milli-gamma (nT).

It should be noted that recently the numerous cases of electrostatic waves with frequencies below the local electron gyrofrequency have been found by the Dynamic Explorer (DE) satellite experiment, although the locations of observation are different, i.e., in the cusp region instead of the inside magnetosphere near equatorial plasmapause shown in the present case (Shawhan, private communication, 1981).

Since the event of emission band broadening took place outside the plasmasphere, where the plasma density is below the order of 100 cm^{-3} (Maynard and Cuaffman, 1973), the resonant energy of the electrons should be higher than 20 keV (for the local gyrofrequency 12 kHz), if the cause of the broadening is assumed to be due to the enhanced anisotropic electrons of resonance with whistler mode waves. This type of emission band broadening has been discussed previously (Maeda and Lin, 1981), and another example is shown in Figure 6 for comparison. As can be seen from the electron data shown in the next section, the behavior of electrons during the burst type emission band spreading is quite different from those of gradual whistler mode spreading. It should also be noted that the frequencies of the broadened band of emission are above the local lower hybrid resonance frequency in contrast to those of the magnetospheric hiss.

4. ELECTRON DATA

The enhancements of ring-current electrons, corresponding to these emissions can be seen from Figure 3, in which the directional differential intensities of electrons from the lowest energy channel (1.01-1.37 keV) to the highest energy channel (240-560 keV) are plotted against UT for the period from 2300 UT on 1st April to 0500 UT on 2nd April, 1972. The electron data below 30.23 keV are obtained by the channeltrons and those above 35 keV are by the solid state electron detectors (Longanecker and Hoffman, 1973). The time interval indicated by horizontal bar-hatching corresponds to that of VLF emission, and those indicated by stippling are the intervals when the satellite is in the plasmasphere.

The characteristics of the temporal variation of the enhanced electrons differ from those of usual VLF emission events in the following way: (1) the rise-time of the enhancement is very short, i.e., the increase of electron intensities is almost instantaneous, (2) there is no velocity dispersion in the onset of the enhancement in contrast to the usual emission events (Maeda et al., 1978), i.e., the enhancement is simultaneous from the lowest energy 1.01-1.37 keV up to 11.74-15.93 keV, (3) no significant enhancements are detected above 20 keV, (4) the duration of the enhancement is less than a few minutes in contrast to the gradual broadening events which continue for hours (Maeda and Lin, 1981), and (5) no significant spreading of the anisotropy appears at high energies.

The last point is illustrated in Figure 4. In this figure, the ratio of electron intensities with pitch angle 90° to those with 27°, the intensity of the smallest observable pitch angle in the data, is plotted against the energy of the enhanced electrons. The data points marked by small open circles and crosses stand for the 5 minutes mean values for the time intervals 0405-0410

UT and 0411-0416 UT, respectively. The former corresponds to the period when the emission is narrow and the latter corresponds to that of broad band emission.

5. DISCUSSION

5.1 Comparison with the Gradual Broadening Events

In the case of gradual broadening emission, the corresponding enhanced electrons show the spreading of its pitch angle anisotropy toward higher energies. Since the production of lower frequency emission requires the large Doppler shift from the electrons which gyrate always with electron cyclotron frequency, f_H, proportional to the local magnetic field intensity, the shift of the resonant electrons from low to higher energies is consistent with the spreading of the emission band towards lower frequencies.

To see the similarities in the locations of both types of the broadband emission events, and the correspondence between the temporal variations of the emission band and anisotropic electron enhancement for other events the following figures for the gradual broadening events are produced for comparison: Figure 5, location of the gradual broadening emission event which was observed along the orbit 421 on 29 March 1972; Figure 6, VLF emission data showing the gradual emission band broadening which started around 2240 UT until 2322 UT when the satellite entered into the nightside plasmasphere; Figure 7, associated enhancements of the electron intensities and anisotropies for the same energy channels as shown in Figure 3; and Figure 8, an indication of the spreading anisotropies toward the higher energies during the event, in the same manner as Figure 4, i.e., the small open circles and a dashed-line are 10 minutes mean values for 2240-2250 UT and cross-marks and full-line are those for 2310-2320 UT.

When the time dependence of the observed electron energy spectra and pitch angle distributions are expressed in analytic form, the gradual spreading of whistler mode emission (such as shown in Figure 6), can be computed. The calculations were performed for the event observed by the S^3-A satellite during a geomagnetic storm on 17 December 1971. Although the absolute value of the wave growth rates due to the cyclotron instability decreases with time because of the decreasing number density of the resonant electrons, the broadening of the frequency dependent growth rates of the waves are quantitatively in good agreement with observed values (Maeda and Lin, 1981). It should be noted that the location of these emissions has been known to be the domain of low density cold plasma during the period of the plasmasphere contraction, following geomagnetic disturbances (Etcheto and Block, 1978). On the other hand, in the case of burst type broadening emission events (the event on the orbit #431), the shift in the electron anisotropy to higher energy did not take place. Furthermore, a sudden enhancement of low energy electron intensity below the order of 10 keV without velocity dispersion as shown in Fig. 3 indicates that the inner edge of plasma sheet, the source of these ring current electrons, was relatively close to the nightside plasmapause in this event.

In these respects, the mechanism of the frequency band broadening of this event is different from the gradual broadening events discussed previously, and the generation of quasi-electrostatic wave of the whistler mode by the a two component plasma instability seems to be one of the plausible mechanisms.

5.2 Emission Band Broadening by Hot Bi-Maxwelliam Electrons.

Since the emission of the burst type broadening event observed on the orbit 431 of Explorer 45 is quasi-electrostatic, the source of free energy for this emission can be found in the relatively low energy electrons with weak

temperature anisotropy, streaming into the magnetized cold plasma.

The characteristics of this two component plasma can be described by adding a bi-maxwellian electron term to the normal (cold) whistler wave dispersion equation (Stix, 1962; Scharer and Trivelpiece, 1967; Hashimoto, 1980), i.e.,

$$c^2k^2 - \omega^2 - \Sigma_s \Pi_s^2 \int_{-\infty}^{\infty} dv_z \int_0^{\infty} dv_\perp \pi v_\perp^2 \cdot \left[(\omega - kv_z)\frac{\partial f_s}{\partial v_\perp} + kv_\perp \frac{\partial f_s}{\partial v_z}\right)(\omega - kv_z - \Omega)^{-1} = 0 \qquad (5.1)$$

where ω , k, and c are angular frequency, wave number of the waves in the plasma and light velocity, respectively.

Π_s: the plasmafrequency with s=c for cold electrons and s=h for hot electrons

Ω: electron cyclotron angular frequency.

The distribution function f_s can be written

$$f_{s=c} = \frac{1}{2\pi v_\perp} \delta(v_\perp)\,\delta(v_z) \qquad (5.2)$$

and

$$f_{s=h} = \frac{1}{\pi V_{T\perp}^2 V_{Tz}} \exp\left[-\left(\frac{v_\perp}{V_{T\perp}}\right)^2 - \left(\frac{v_z}{V_{Tz}}\right)^2\right] \qquad (5.3)$$

where

$$V_{T\perp} = \sqrt{\frac{2kT_\perp}{m}} \text{ and } V_{Tz} = \sqrt{\frac{2kT_z}{m}}$$

$kT_\perp$, kT_z and m are kinetic energies of hot electron corresponding to the normal and parallel components of the temperature with respect to the static magnetic field, and the rest mass of electrons (these are expressed in keV), respectively.

Substitution of (5.2) and (5.3) into (5.1) gives the following dispersion formula,

$$c^2k^2 - \omega^2 - \frac{\Pi_c^2 \omega}{\Omega - \omega} - \Pi_h^2 \cdot \frac{\omega Z(\alpha)}{kV_T} + A\,[1 + \alpha Z(\alpha)] = 0 \qquad (5.4)$$

where

$$A = \frac{T_\perp}{T_z} - 1 \quad , \text{ and } Z(\alpha) \text{ is the plasma function defined by}$$

$$Z(\alpha) = \frac{1}{\sqrt{\pi}} \int_{-\infty}^{\infty} \frac{e^{-t^2}}{t-\alpha}\, dt, \qquad \alpha = \frac{\omega-\Omega}{kV_{Tz}} \tag{5.5}$$

Solving (5.4) with respect to $\omega = \omega_r + i\gamma$ the following growth rate of the wave can be obtained,

$$\frac{\gamma}{\Omega} = \sqrt{\pi}\, \frac{\Pi_h^2}{\Pi_c^2} \frac{(1-x)^2}{y} [A - (A+1)x] \exp\left[-\left(\frac{1-x}{y}\right)^2\right] \tag{5.6}$$

where $x = \frac{\omega_r}{\Omega}$ and $y = \frac{kV_{Tz}}{\Omega}$.

The normalized growth rate γ/Ω is plotted in Figure 9 against the normalized frequency, x ($= f/f_H$) with a parameter y. Since no measurement of the plasma density has been made by the S^3-A satellite, the ratio Π_h^2/Π_c^2 is assumed to be 0.1 and $A = 1.5$ in the present calculation. The figure shows that the maximum of the growth rate of the emission shifts toward lower frequency with increasing parameter $y = \frac{kV_{Tz}}{\Omega}$. In turn, y increases with increasing V_{Tz} or k for constant Ω. As indicated in Figure 3, the enhancements of electron intensities are limited below the order 10 keV during the emission band broadening. The broadened band emissions can therefore, be consistent with waves of large k. i.e., shorter waves. This is consistent with the observations indicating that the broadened emissions are not long wavelength whistler waves but are quasi-electrostatic. The growth rate increases with the ratio of hot electron density to that of cold electrons, $\frac{\Pi_h^2}{\Pi_c^2} = \frac{N_h}{N_c}$ which suggests that the source location is in a region of low density cold plasma. The present calculation based on Eq. (5.6) is, however, not applicable to the case $\frac{\Pi_h^2}{\Pi_c^2} \gtrsim 1$.

6. CONCLUSION

In contrast to the gradual broadening of the VLF emissions associated with gradual shifts of anisotropy of the enhanced ring current electrons to higher energies with time, the burst type broadened emissions are quasi-electrostatic, which can be produced by the two-component plasma instabilities where the free energy is bi-maxwellian hot electrons. Energies of the hot electrons are below the order of 1 keV, which are injected into the low density magnetized cold plasma from the plasma sheet during the event.

The main difference of the burst type broadening emission event from the more frequently observed gradual broadening emissions is, therefore, the closeness of the hot electron source, i.e., the close inner edge of the plasma sheet to the nightside plasmapause.

Acknowledgements

A. C. electric field data, magnetic field data in the present investigation are provided by Prof. D. A. Gurnett, University of Iowa and Prof. L. J. Cahill, University of Minnesota, respectively. The electron data are obtained from the experiments performed by Dr. R. A. Hoffman, NASA and Dr. D. J. Williams, NOAA. The computer analysis and plottings are made available by Chris Gloeckler, Goddard Space Flight Center.

I wish to thank Dr. Wynne Calvert, University of Iowa, who kindly provided the wideband VLF emission data discussed in this paper.

References

Anderson, R. R. and D. A. Gurnett, Plasma wave observations near the plasmapause with the S^3-A satellite, J. Geophys. Res., 78, 4756-4764, 1973.

Anderson, R. R. and K. Maeda, VLF emissions associated with enhanced magnetospheric electrons, J. Geophys. Res., 82, 135-146, 1977.

Burtis, W.J. and R.A. Helliwell, Banded Chorus: A new type of VLF radiation observed in the magnetosphere by OGO 1 and OGO 3., J. Geophys. Res., 74, 3002-3010, 1969.

Burtis, W.J. and R.A. Helliwell, Magnetospheric Chorus: Occurrence patterns and normalized frequency, Planet. Space Sci., 24, 1007-1024, 1976.

Etcheto, J. and J. J. Block, Plasma density measurements from the GEOS-1 relaxation soundes, Space Sci. Rev., 22, 597-610, 1978.

Hashimoto, K., Propagation and instabilities of obiquely propagating whistler mode waves in a hot magnetospheric plasma, Ph. D. Thesis Kyoto University, 1980.

Kivelson, M.G., and D.J. Southwood, Local time variations of particle flux produced by an electrostatic field in the magnetosphere, J. Geophys. Res., 80, 56-65, 1975.

Lincoln, J. V. Geomagnetic and Solar Data, J. Geophys. Res., 77, 4280, 1972.

Longanecker, G. W. and R. A. Hoffman, S^3-A spacecraft and Experiment description, J. Geophys. Res., 78, 4711-4717, 1973.

Maeda, K., Cyclotron side-band emissions from ring-current electrons, Planet. Space Sci., 24, 341-347, 1976.

Maeda, K., P.H. Smith, and R.R. Anderson, VLF emission from ring-current electrons, Nature, 263. 37-41, 1976.

Maeda, K., N.K. Bewtra and P.H. Smith, Ring current electron trajectories associated with VLF emissions, J. Geophys. Res., 83, 4339-4346, 1978.

Maeda, K. and C.S. Lin, Frequency band broadening of magnetospheric VLF emissions near the equator, J. Geophys. Res., 86, 3635-3639, 1981.

Maynard, N. C. and D. L. Cauffman, Double floating probe Measurements on S^3-A, J. Geophys. Res., 78, 4745-4750, 1973.

Scharer, J. E. and A. W. Tivelpiece, Cyclotron wave instabilities in a plasma, Phys. Fluids, 10, 591-595, 1967.

Parady, B. K., D. D. Eberlein, J. A. Morris, W. W. L. Taylor and L. J. Cahill, Jr., Plasmaspheric hiss observations in the evening and afternoon gradients, J. Geophys. Res., 80, 2183, 1975.

Southwood, D.J. and M.G. Kivelson, An approximate analytic description of plasma bulk parameters and pitch angle anisotropy under adiabatic flow in a dipolar magnetospheric field, J. Geophys. Res., 80, 2069-2073, 1975.

Stix, T. H., The theory of plasma waves, McGraw-Hill New York, 1962.

Tsurutani, B.T., and E. Smith, Postmidnight chorus: A substrom phenonmenon, J. Geophys. Res., 79, 110-127, 1974.

Figure Captions

Figure 1. The orbit 431 of the S^3-A satellite (Explorer 45). The dashed lines with P.P. are plasmapauses and shaded domain is the plasmasphere. A mark on the inbound orbit just outside of the plasmasphere is the location of the broad band VLF burst event.

Figure 2. Wideband VLF emission data obtained by the Explorer 45 on April 2, 1972. The upper and lower panels correspond to the AC magnetic field and electric field intensities with the upper cut-off at 3 kHz and 10 kHz, respectively.

Figure 3. The differential directional electron intensities measured by the Explorer 45 for the period from 2300 UT of April 1 to 0530 UT on 2 April in 1972. The time intervals indicated by stippling is the period when the satellite is in the plasmasphere. A time interval indicated by horizontal lines corresponds to the period of VLF-broad band burst. Energies of electrons are from 1.01 - 1.37 keV for the bottom curve and 240-560 keV at the top. Crosses and open-circles correspond to the pitch angle 90° and 27° respectively.

Figure 4. The electron intensity anisotropy parameter, $j_\perp/j_\parallel$ plotted against energies of electron (in keV). Open circles and cross marks correspond to the 5 min average of electron data shown in Fig. 3, when the emission band is narrow (0405-0410 UT) and broadened (0411-0416 UT), respectively. A dashed line

and a full line are polynomial approximation for narrow band and broad band period, respectively, using all data points but truncated at the 2nd term.

Figure 5. The orbit 421 of Explorer 45, indicating the location of the gradual broadening emision along inbound orbit. All notations are the same as Figure 1.

Figure 6. The wideband data of gradual broadening VLF-emission observed on 29 March 1981 along the orbit 421 of the S^3-A satellite. Notations are the same as those of Figure 2.

Figure 7. The differential directional intensities of electrons plotted against UT on 29 March 1981. All notations are the same as those used in Figure 3.

Figure 8. The same as Figure 4 except for the electron data of 29 March 1972 shown in Figure 7. Open circles and cross marks are 10 min average for the time interval 2240-2250 UT (narrow band period) and for 2310-2320 UT (broad band period), respectively.

Figure 9. The normalized growth rate, $\frac{\gamma}{\Omega}$, of emissions below the electron cyclotron frequency f_H in the two component plasma versus the normalized frequency $x = f/f_H$.

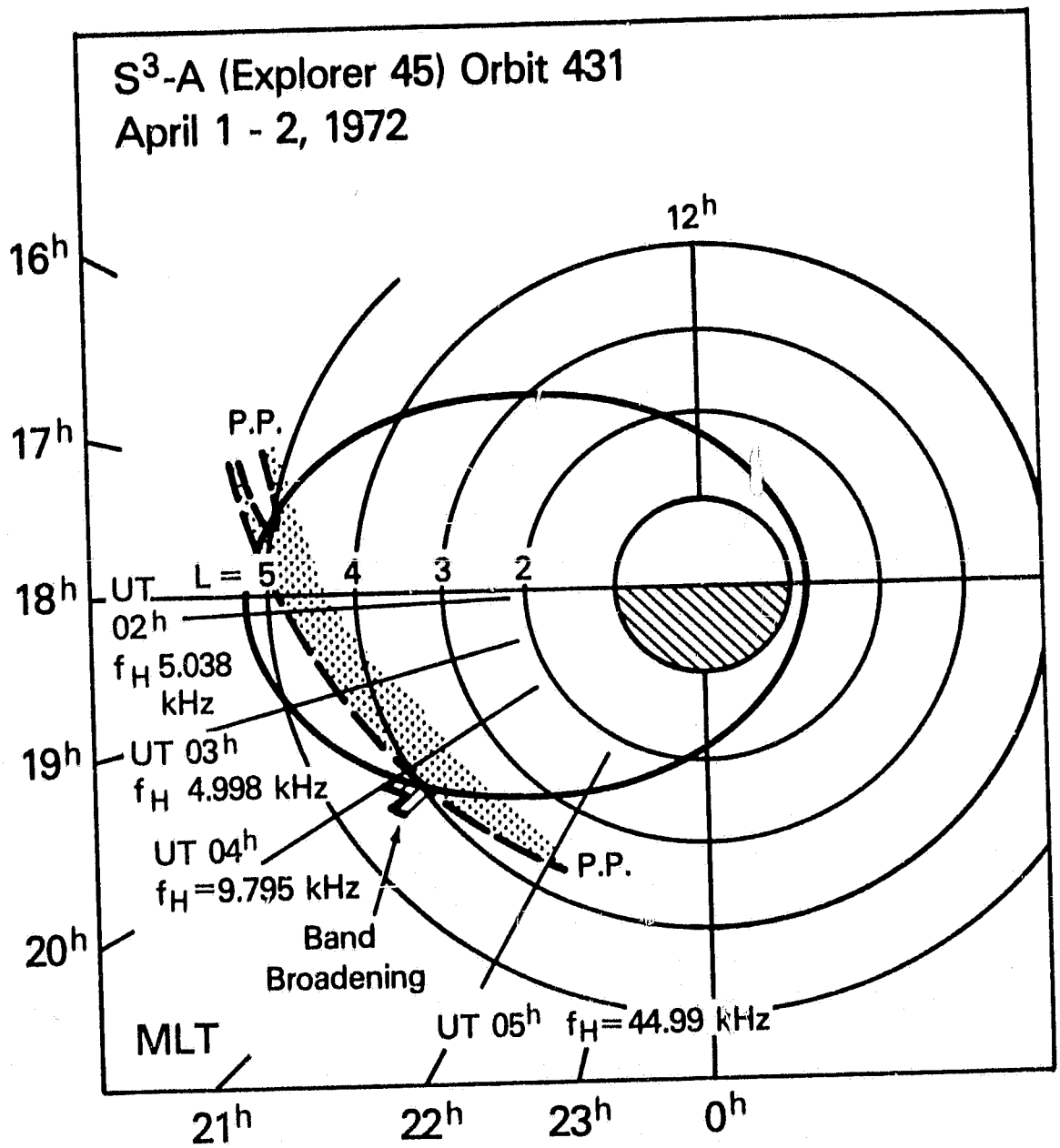

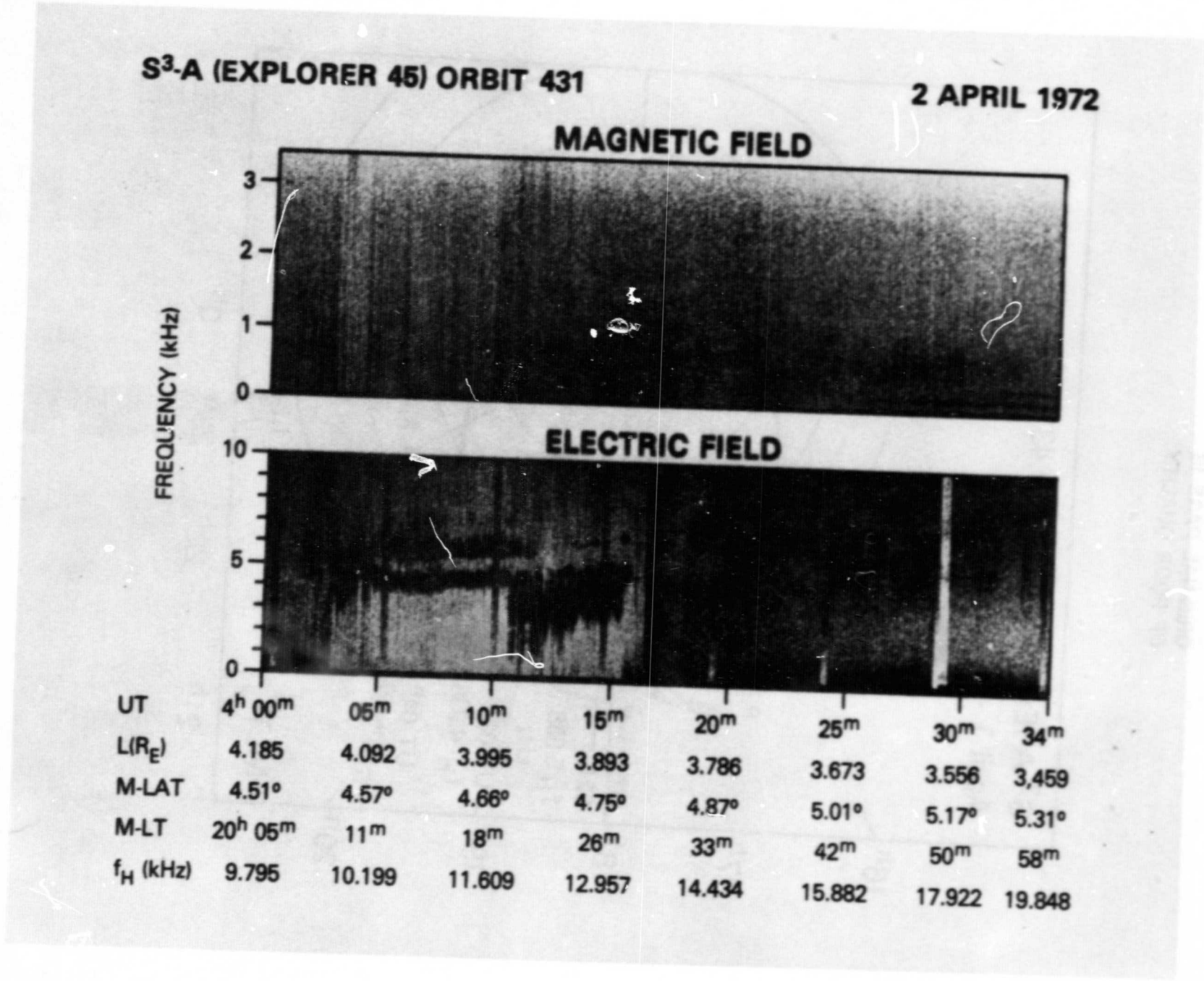

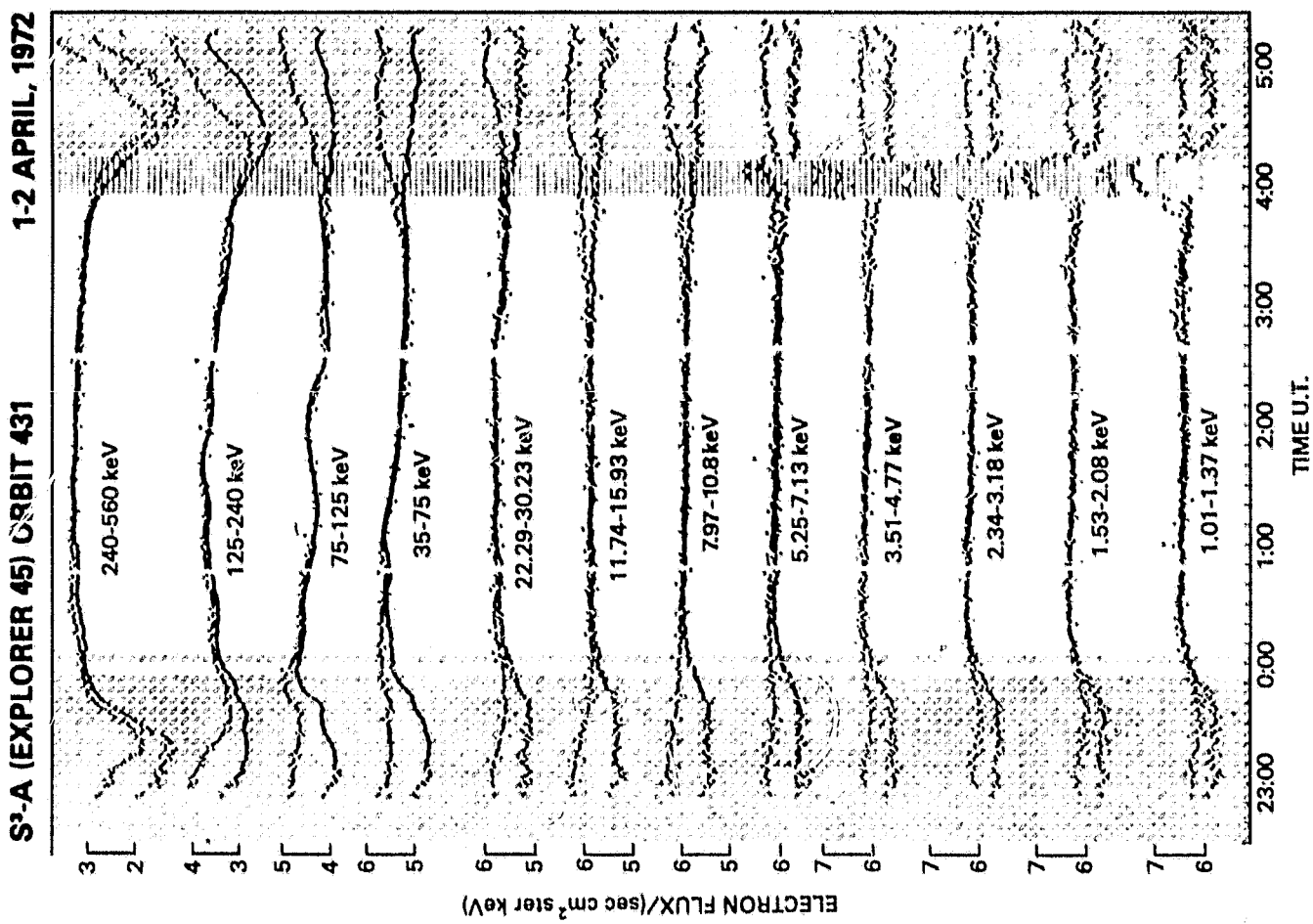

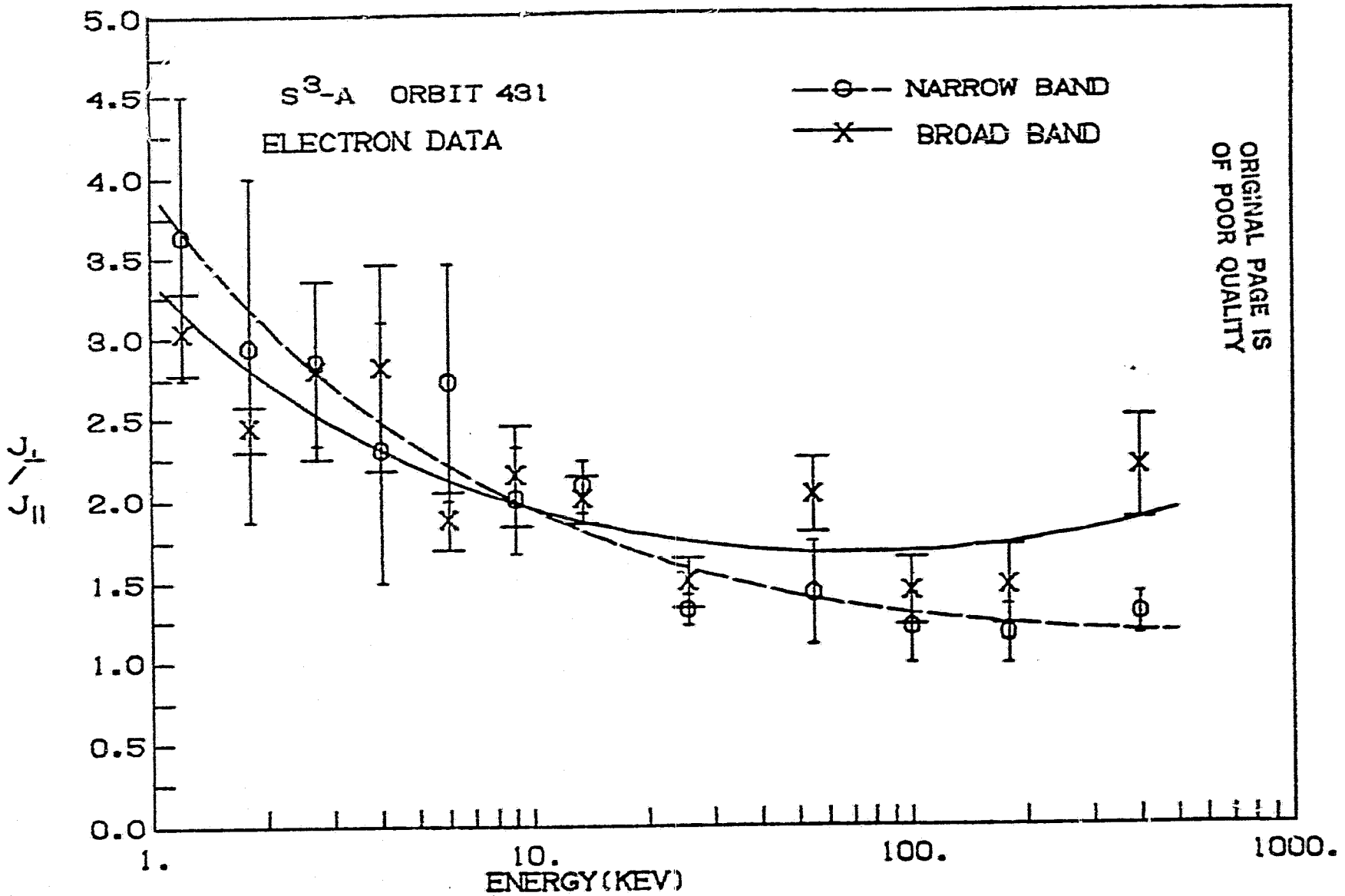
S3-A ORBIT 431
ELECTRON DATA
NARROW BAND
BROAD BAND
ORIGINAL PAGE IS
OF POOR QUALITY
J⊥ / J∥
5.0
4.5
4.0
3.5
3.0
2.5
2.0
1.5
1.0
0.5
0.0
1.
10.
100.
1000.
ENERGY(KEV)

S^3-A (EXPLORER 45) ORBIT 421
29 MARCH, 1972

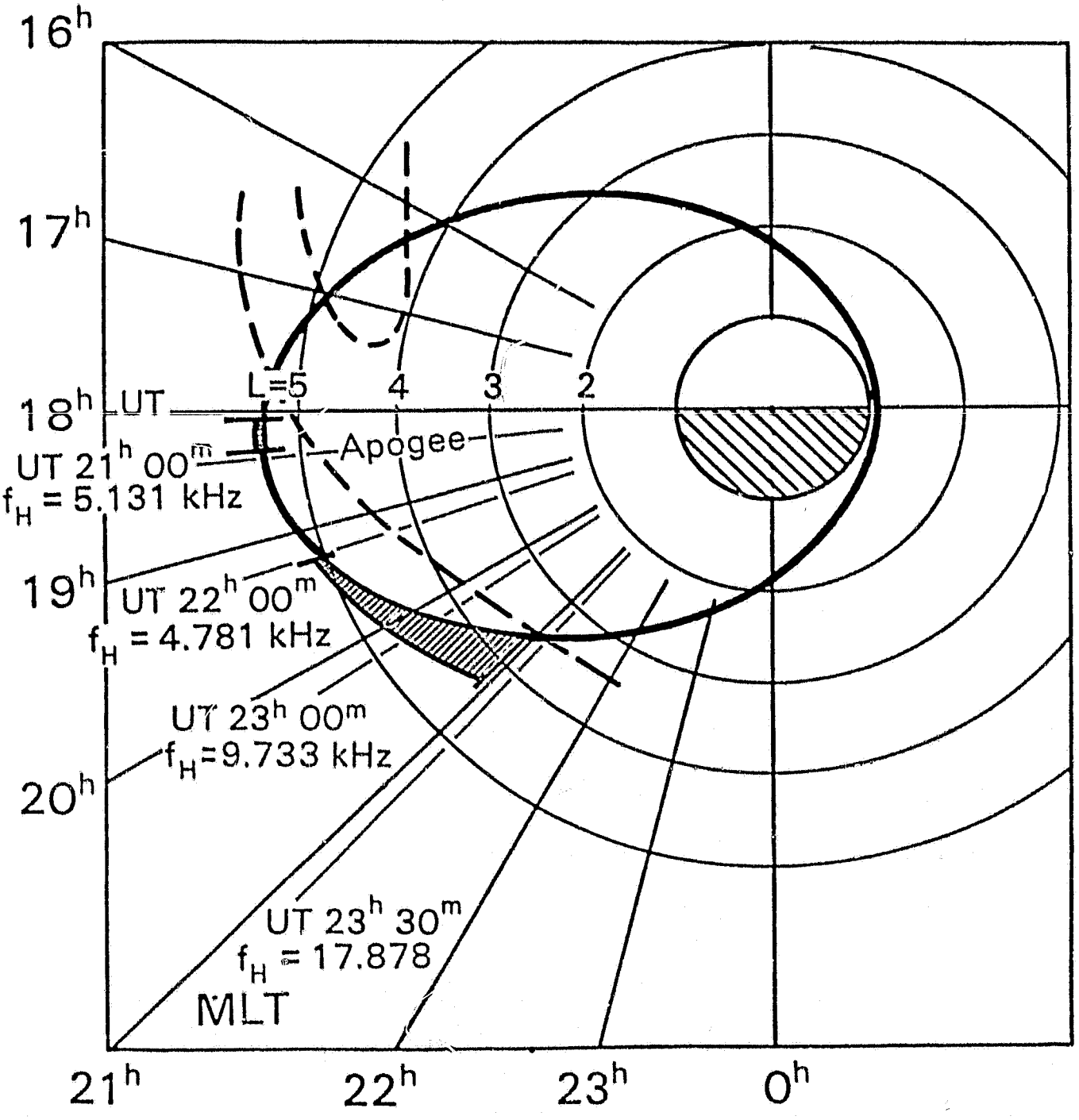

S^3-A (EXPLORER 45) ORBIT 421 29 MARCH 1972

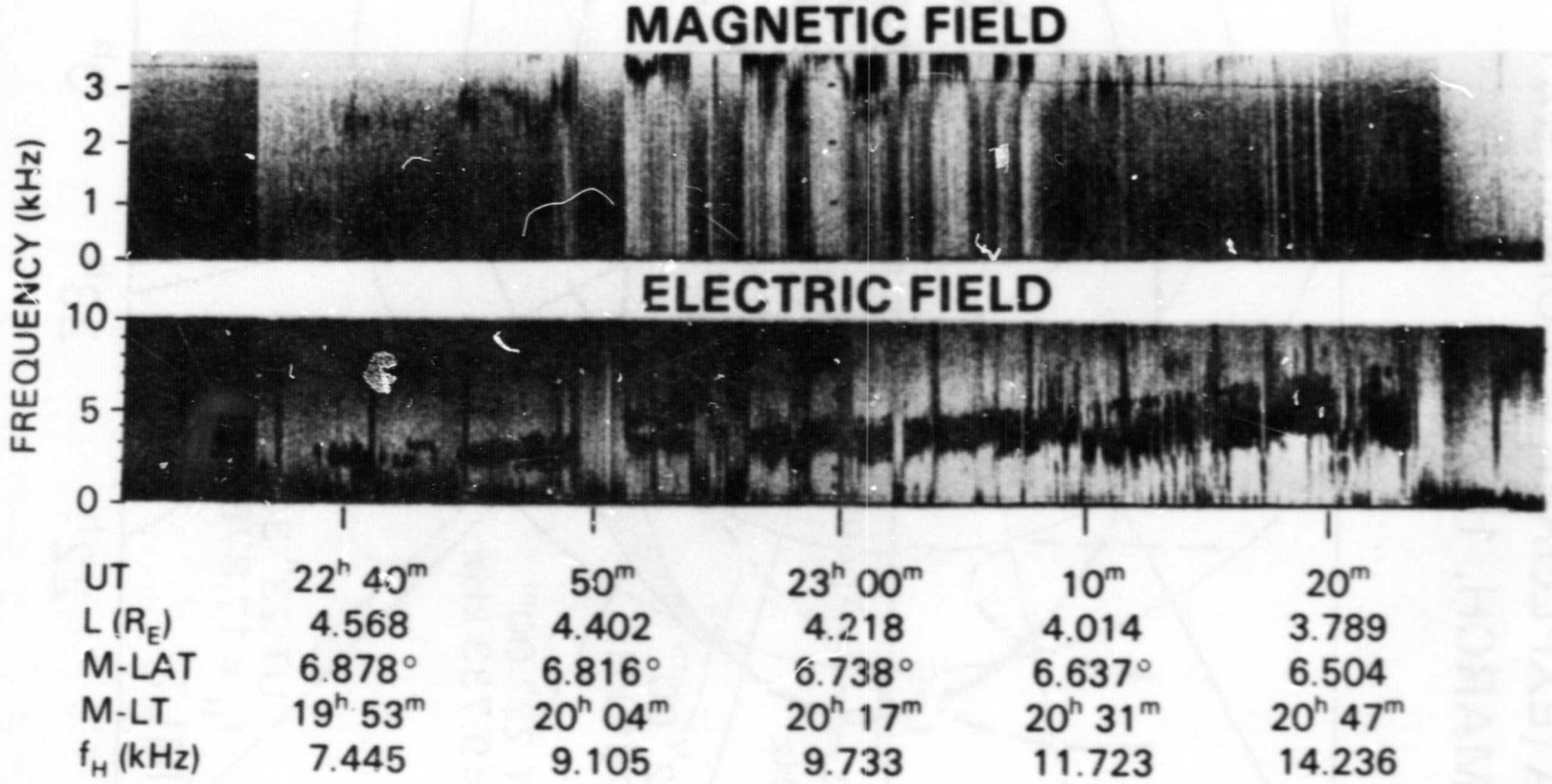

UT	$22^h\ 40^m$	50^m	$23^h\ 00^m$	10^m	20^m
L (R_E)	4.568	4.402	4.218	4.014	3.789
M-LAT	6.878°	6.816°	6.738°	6.637°	6.504
M-LT	$19^h\ 53^m$	$20^h\ 04^m$	$20^h\ 17^m$	$20^h\ 31^m$	$20^h\ 47^m$
f_H (kHz)	7.445	9.105	9.733	11.723	14.236

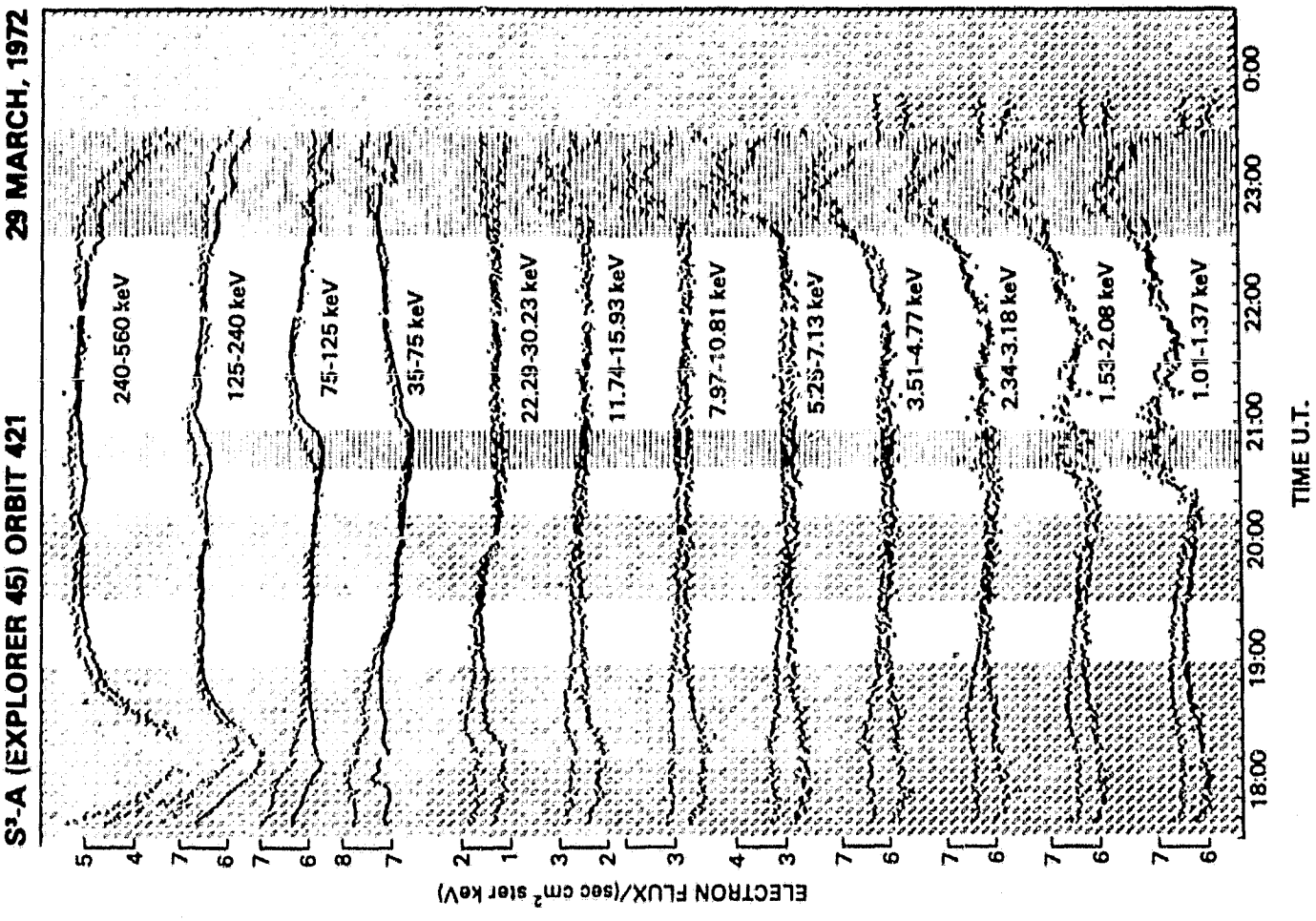

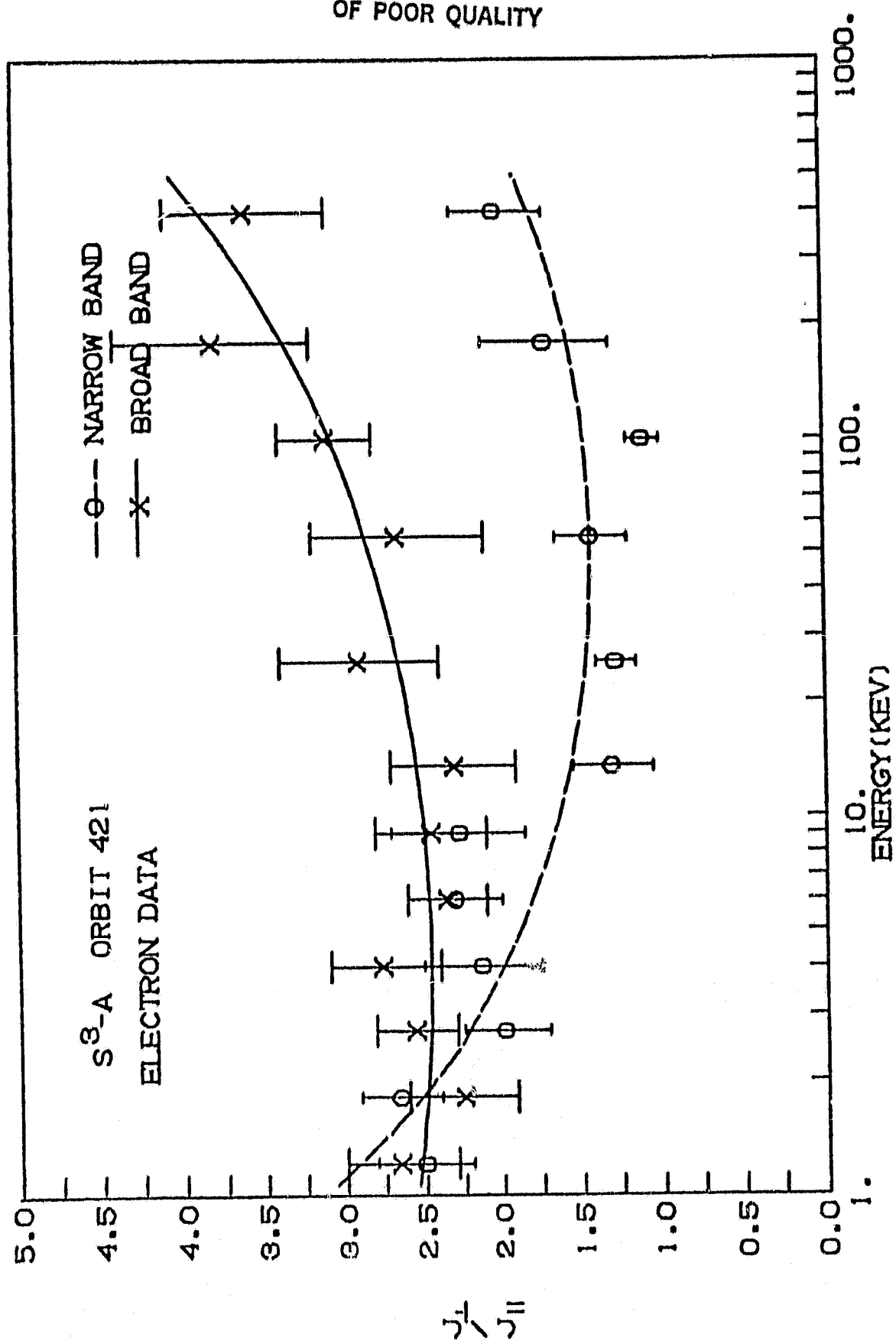

ORIGINAL PAGE IS
OF POOR QUALITY